Absolute refractometry of dry gas to ± 3 parts in 10^9

Patrick Egan and Jack A. Stone*

National Institute of Standards and Technology, 100 Bureau Drive, Gaithersburg, Maryland 20899, USA

*Corresponding author: jack.stone@nist.gov

We present a method of measuring the refractive index of dry gases absolutely at 632.8 nm wavelength using a Fabry–Perot cavity with an expanded uncertainty of $<3 \times 10^{-9}$ (coverage factor $k = 2$). The main contribution to this uncertainty is how well vacuum-to-atmosphere compression effects (physical length variation) in the cavities can be corrected. This paper describes the technique and reports reference values for the refractive indices of nitrogen and argon gases at 100 kPa and 20 °C with an expanded uncertainty of $<9 \times 10^{-9}$ (coverage factor $k = 2$), with the additional and larger part of this uncertainty coming from the pressure and temperature measurement.

OCIS codes: 120.3940, 120.2230, 120.5710, 140.3425.

1. Introduction

All length measuring interferometers rely on optical wavelength for scale, but the accuracy of air-based interferometers is only as good as the knowledge of the refractive index of air. For decades the refractive index of air has been estimated using empirical equations relating refractive index to pressure, temperature, humidity, and carbon dioxide content [1–5], but even the most precise measurements of these environmental conditions (that is, employing a weather station) will give an estimate of refractive index no better than a few parts in 10^8. In practice, uncertainty in the refractive index of air often contributes a yet larger uncertainty to the highest accuracy air-based displacement measurements [6] and dimensional calibrations [7,8].

Fabry–Perot (FP) cavities offer a precise method of determining gas refractive index directly [9–12]. A laser is in resonance with an FP cavity when an integer number m of half-wavelengths $\lambda/2$ equals the cavity length L; which is to say, the wavelength of a cavity mode is $\lambda \approx 2L/m$. The optical frequency of a cavity mode—a resonant frequency—is $\nu \approx mc/(2nL)$, where c is the speed of light in vacuum and n is the refractive index of the medium between the cavity mirrors. When a laser is servolocked to a resonant frequency of a dimensionally stable cavity, its wavelength is fixed and the frequency of the laser will track the changes in refractive index: $\frac{d\nu}{\nu} \approx -\frac{dn}{n}$.

This approach can be extended to measure refractive index absolutely: a resonant frequency is measured when the cavity is first at vacuum ($n = 1$) and a second resonant frequency is measured when the cavity is filled with gas at, say, atmospheric pressure. To determine the absolute refractive index of the gas, in addition to the resonant frequencies, the change in the cavity mode number m going from vacuum to atmospheric pressure must be known, along with the pressure-induced length distortions of the cavity. If the distortions are corrected for using helium [13], then, in theory, absolute refractometry with FP cavities could reach accuracy levels of 10^{-10}. Practical issues, such as helium purity, thermometry, and pressure measurement preclude this level of accuracy at present, but, as we report, absolute refractometry with FP cavities could outperform weather stations by an order of magnitude.

We would envision replacing weather stations on the most accurate air-based dimensional measuring machines at the National Institute of Standards and Technology with FP cavity refractometers, thereby effectively eliminating contributions from air refractive index to length measurement uncertainty. The cavities would be made from dimensionally stable, low thermal expansion material, with the length of the cavity calibrated periodically at vacuum. In our efforts to implement this plan, we have characterized two FP cavities of different lengths and evaluated

their suitability for air refractometry. These tests revealed a problematic sensitivity in the cavity and/or mirror coatings to humidity; at the present time, we cannot claim that we can measure the refractive index of moist air absolutely to any better than 2×10^{-8}. That being said, the expanded uncertainty of the refractometer in dry gas at atmospheric pressure was $<3 \times 10^{-9}$ ($k = 2$), and we now describe the system and report the most accurate reference values to date for the refractive indices of nitrogen and argon gases at a wavelength of 632.8 nm.

2. Method and Apparatus

Our refractometry system is built around a plano-concave FP cavity and measuring its resonant frequencies when the cavity is at vacuum and filled with gas. Achieving this requires the optics and electronics to lock a laser to a resonant frequency of the cavity, and the ability to measure this resonant frequency absolutely. Vacuum and gas line plumbing are also necessary, and temperature and pressure around the cavity must be controlled and measured with high accuracy. Our setup consists of two independent systems for measuring refractive index that are mounted next to each other so that they can be compared. As shown in Fig. 1, two FP cavities of substantially different lengths are mounted in a vacuum chamber within a thermally controlled box. For clarity, only one laser system is shown; in actuality, we had two identical laser systems, frequency-modulated differently. For general operation, one laser was locked to each cavity and its absolute frequency was measured by beating against an iodine-stabilized He–Ne laser, but we also had the possibility of coupling both lasers into the same

Fig. 1.   (Color online) Optical setup for refractometry (only one laser system is shown). Components include: thermally tunable helium–neon laser (He–Ne), isolators (iso), polarizing beamsplitter (pbs), acoustooptic modulator (aom), mirrors (m), lenses (pcx, bcx), fiber coupler/collimator (fc), polarization-maintaining single-mode fiber (pm-smf), nonpolarizing beamsplitters (bs), 100 kHz photodetectors (pd), and 1 GHz avalanche photodetector (apd). End-on photograph of longer FP cavity also shown.

optical fiber so as to measure the free spectral range (FSR) of each cavity.

A.   Optics and Electronics

We locked the lasers to the FP cavities using the frequency dither technique: a lock-in amplifier, a photodetector, and two proportional–integral–derivative (PID) controllers locked the laser wavelength to the cavity resonance. The lock-in amplifier was used for phase-sensitive detection of the photodetector signal, synchronous with frequency modulation provided by the double-pass acoustooptic modulator (AOM). The dither frequency was about 65 kHz for one laser and about 86 kHz for the second laser. The amplitude of the dither was chosen so as to give a peak frequency deviation approximately equal to the cavity transmission linewidth (about 2 MHz). Each lock-in amplifier output was fed into two PID controllers working in series, one dedicated to fast, and the other to slow, laser frequency control. The fast controller servoed the frequency of the double-pass AOM with a tuning range of 20 MHz and bandwidth of 16 kHz. The slow controller followed the fast controller and servoed an internal heater on the laser tube giving a tuning range of 1.2 GHz and bandwidth of 0.2 Hz. About 40 μW of laser power reached the cavity and the coupling efficiency was close to 50%. The absolute resonant frequency of each cavity was measured by beating the laser beam reflected from the cavity against an iodine-stabilized He–Ne laser (measurement uncertainty <5 kHz). At least 20 μW of laser power was incident on the avalanche photodetector and the signal-to-noise ratio of the beat frequencies was at least 35 dB in a resolution bandwidth of 300 kHz. In practice, we separately bandpass filtered and measured (a) the beat frequency of one cavity resonance against an iodine line and (b) the beat of one cavity resonance against the other cavity (intercavity beat), simultaneously with separate frequency counters. For self-consistency and determining sign, we also briefly noted the beat frequencies of each cavity with two separate iodine lines.

The FP cavities (both spacer and end mirrors) were made of ultralow expansion (ULE) glass [14], and the end mirrors were optically contacted (Van der Waals bond) to the spacer. The salient property of ULE that makes it desirable for absolute refractometers is its long-term dimensional stability [15] compared to other low thermal expansion materials [12,16]. However, ULE has the disadvantage that it absorbs helium, as will be discussed shortly. It is also desirable that the spacer and end mirrors are made of the same material to avoid internal stresses and distortion of the mirrors arising from temperature and pressure changes [13,17]. Both cavities had a coefficient of thermal expansion of 3×10^{-9} K^{-1} over the range 19.5 °C to 20.5 °C, with a temperature of zero expansion close to 19.0 °C. The spacers had a square cross section of width 60 mm and a rectangular slot of width 8 mm, and depth 35 mm was cut lengthwise (see end-on photograph of one FP cavity in Fig. 1).
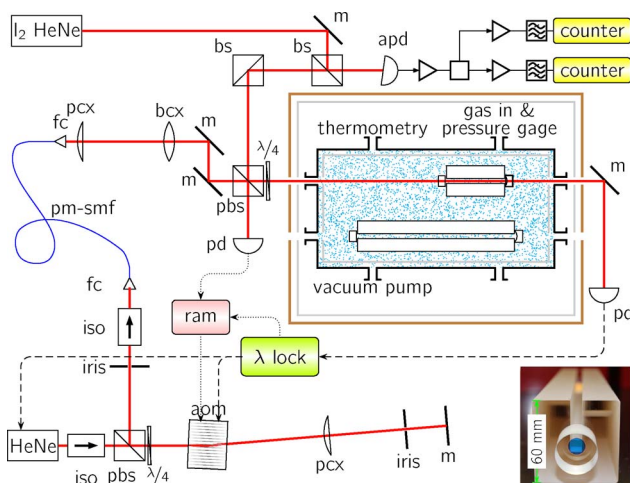
The slot running the entire length of the cavity helped to assure that the gas in the cavity was in equilibrium with its surroundings. The lengths of the spacers were 143 and 329 mm. The back surfaces of the mirror substrates were antireflection-coated, wedged at 1°, and contacted to the spacer antiparallel to one another. The mirrors were claimed to have a maximum reflectivity of 99.7% at 622 nm (the effect of mirror dispersion on phase shift when used at 632.8 nm will be addressed shortly). We measured both the transmission linewidth and the FSR of each cavity to estimate finesses of about 400. This relatively low cavity finesse can be desirable because it will not change dramatically when exposed to a laboratory environment with less than perfect cleanliness. If the finesse were state-of-the-art (exceeding 10^5), there would be a danger that locking characteristics might substantially change due to contamination of the mirror surface when used in a typical measurement environment, and cleaning the mirrors could be problematic; for these reasons we chose a low-finesse cavity design. However, locking to a low-finesse cavity is more sensitive to electronic offsets and residual amplitude modulation (RAM).

Accurate knowledge of the FSR plays a central part in determining the gas refractive index in our technique, as will soon be discussed. To measure the FSR—the difference between adjacent resonant frequencies—of a cavity to better than 10^{-3} of a cavity linewidth, it was necessary to suppress the RAM present on the dithered laser [18]. The RAM arises because the diffraction efficiency of the double-pass AOM varies with its rf driving frequency; also, imperfect setup of the double-pass AOM can cause frequency-dependent steering effects at the modulation frequency and harmonics thereof, and this will generate RAM when the beam is coupled to an optical fiber. The problem with RAM is that it introduces an offset into the electronic lock point, which, in turn, leads to a frequency offset when determining the FSR. This error in FSR may not reveal itself in the stability of the beat frequency between adjacent modes of the same cavity, and can be investigated at the $<10^{-3}$ of a cavity linewidth level by locking two lasers to combinations of different modes in the same cavity. To monitor RAM, about $2\,\mu\text{W}$ of laser power was directed onto a photodetector immediately before entering the vacuum chamber (see Fig. 1), and an out-of-loop lock-in amplifier referenced to the dither frequency measured the RAM present on the laser. Without suppression, RAM was present at the 1% level, which produced errors in the measurement of an FSR of 7 kHz (note, the stability of an FSR beat frequency without RAM suppression was on the order of 100 Hz). We suppressed RAM to 0.01% by modulating the driving voltage of the AOM synchronously with the dither signal (scaled and phase-shifted); modulating the driving voltage of the AOM modulated the intensity of the laser at its dither frequency so as to suppress the RAM.

The uncertainty of the FSR measurement for the long cavity was evaluated by locking the lasers to combinations of different modes, separated by one or two FSRs, to build a vector of six unique FSR measurements. With RAM suppressed, we obtained a best FSR value from the set of six measurements with a 95% confidence interval (based on the t-distribution) of 122 Hz (8 parts in 10^5 of the cavity linewidth). This value can be taken as an estimate of the expanded uncertainty (thus, 61 Hz standard uncertainty). For the short cavity, the limited tuning range of the lasers only allowed locking to two modes. Based on the spread of the two FSR measurements, we conservatively estimated the standard uncertainty to be 250 Hz. (The relative uncertainty of the FSR measurement would be expected to be the same for both cavities, so that the 61 Hz uncertainty for the long cavity would scale to 140 Hz for the short cavity.) The Allan deviation in the beat frequency between two lasers locked to adjacent modes of the same cavity was about 10 Hz with a 100 s averaging time. Although this laser locking performance is rather good for a low-finesse cavity, it came at the additional effort of having to suppress RAM, and in future we would aim for cavities with a finesse closer to 4000 than 400.

B. Pressure and Temperature

Gas pressure and temperature need to be controlled and carefully measured when (a) determining the refractive index of helium from first principles, (b) precisely comparing two refractometers, and (c) establishing reference values for a dry gas at a specified temperature and pressure. The FP cavities were placed in an elastomeric-sealed vacuum chamber with a temperature stabilization system. Before measuring any gas, the vacuum chamber was pumped down to $10^{-2}\,\text{Pa}$ and baked at 60 °C for several days. When either at high vacuum or sealed off with gas at 100 kPa, the outgassing/permeation rate of the system was about 0.05 Pa/h. This level of cleanliness is essential for any serious attempt at absolute refractometry, especially those that calibrate out compressibility effects with helium (the refractivity of helium is almost an order of magnitude less than that of contaminants such as air and water vapor, so even a 1 Pa contamination at atmospheric pressure would limit helium correction to no better than 3×10^{-9}). Pressure was measured with a portable pressure gauge, recently calibrated with a standard uncertainty of 0.5 Pa at 100 kPa, and had a 1.5 Pa hysteresis going from vacuum to atmospheric pressure. The temperature sensitivity of the barometer at 100 kPa was less than 0.1 Pa/K. The pressure gauge was insensitive to gas species and its height relative to the cavities was known to 20 mm. For argon at 100 kPa and 20 °C, this height uncertainty corresponded to a 0.3 Pa uncertainty in gas head correction.

Like pressure, temperature must be measured with the highest possible accuracy. This is most

reliably achieved if spatial and temporal temperature gradients are kept as small as possible in a temperature-stabilized system. The temperature-stabilization system [19] consisted of two stages of aluminum enclosure; one enclosure outside the stainless steel vacuum chamber and one inside. The outer aluminum envelope was stabilized to $1\,\mathrm{mK}$ with a servo of thermistors, foil heaters, and PID control. Gas temperatures near the ends of the two cavities were measured with four type-T thermocouples (inserted into the lengthwise cavity slot) with their reference junctions inserted into a copper block whose temperature was monitored with a thermistor thermometer system. The copper block projected into the vacuum chamber. The thermistor had been recently calibrated with a standard uncertainty of $1\,\mathrm{mK}$. We consider this calibration uncertainty to be the largest source of uncertainty in temperature measurement. Critical to verifying accuracy was to show that, if the thermocouple sensing junctions were attached to the outside of the copper block, they all indicated less than a $0.5\,\mathrm{mK}$ temperature difference with the reference junction. This shows both that the reference block is isothermal and that offset emfs (in the nanovoltmeter and switch used for thermocouple measurements) do not produce $>0.5\,\mathrm{mK}$ errors. In general, temperature measurement with submillikelvin uncertainty is much easier in an environment where everything is isothermal within a few millikelvin, as in our situation. For example, uncertainties in the Seebeck coefficient become negligible when the reference junction is within a few millikelvin of the measurement point. Similarly, the disrupting influence of heat transfer via conduction through the thermocouple leads or radiative coupling between the thermocouple sensing element and the surroundings becomes very small when all the surroundings are nearly at the same temperature as the measurement point.

Both cavities were suspended at their Airy points with $0.3\,\mathrm{mm}$ diameter steel cables, and were hung less than $0.7\,\mathrm{mm}$ above a polished $25\,\mathrm{mm}$ thick aluminum plate. The $<0.7\,\mathrm{mm}$ gap was sufficiently small to provide substantial heat transfer between the cavity and the plate; this reduced thermal gradients and expedited thermal equilibration following temperature transients (such as occur when gas is admitted to the chamber, for example).

C. Absolute Refractive Index

The frequency of a laser ν locked to the resonance of an FP cavity of length L is given by

$$\nu = \frac{c}{2nL}\left[m + \frac{\Phi(L)}{\pi} - \frac{\phi_R(\nu)}{2\pi}\right], \qquad (1)$$

where the mode number m is an integer, c is the speed of light in vacuum, and n is the refractive index of the medium between the cavity mirrors. The expression in Eq. (1) accounts for the diffraction phase shift $\Phi(L)$ of the propagating beam and the sum of reflection phase shifts $\phi_R(\nu)$ of the two mirrors. (The notation and development given in this section is largely based on [20]. Notation and terminology differ from what was used in [13].)

Absolute gas refractivity $n-1$ can be estimated from Eq. (1) by measuring the initial resonant frequency ν_i when the cavity is under vacuum and the final resonant frequency ν_f when the cavity is filled with gas and calculating

$$n - 1 = \frac{(\nu_i - \nu_f)(1 + \varepsilon_\alpha) + \Delta m\dfrac{c}{2L_i} + \varepsilon_d}{\nu_f} + n\frac{L_i - L_f}{L_i}, \qquad (2)$$

where Δm is the change in mode number. The final term on the right of Eq. (2) accounts for possible changes in the length of the cavity from L_i to L_f as the cavity is filled with gas. The term ε_d depends on the change in diffraction phase shift when the cavity is brought from vacuum to gas at some final pressure, but ε_d probably has no practical consequences. For a cavity with one flat mirror and one mirror of radius R, the diffraction phase shift $\Phi(L) = \arcsin[(L/R)^{1/2}]$ and thus depends only on the ratio L/R; this ratio is constant unless the cavity anomalously distorts as a function of pressure. If the cavity is built from dissimilar materials, causing it to be subject to significant anomalous distortions, the ε_d term might become big enough to be nonnegligible, but in practice the term can simply be absorbed into a calibration of pressure effects as described later in this subsection. Thus, ε_d can normally be ignored. The term $\varepsilon_\alpha = \alpha c/(4\pi L_i)$ in Eq. (2) accounts for linear dispersion of the phase change in mirror reflection as a function of laser frequency, $\alpha = \mathrm{d}\phi_R/\mathrm{d}\nu$ (for our cavity mirrors $\alpha \approx 10.5/\nu$). The effect of ε_α is of negligible consequence for our measurements, contributing less than 10^{-11} to the measured refractive index. However, ε_α cannot be ignored in a second context, when the vacuum cavity length L_i is determined via measurement of the FSR, utilizing the relationship $\Delta\nu_{\mathrm{fsr}} = \frac{c}{2L_i}/(1 + \varepsilon_\alpha)$. Ignoring ε_α in this context could cause errors as large as 1×10^{-9} in refractive index measurements. Also note that to employ Eq. (2), it is necessary to know the change in mode number Δm. This can be determined in a variety of ways, but perhaps the simplest method is to guess Δm based on approximate knowledge of the refractive index. If the pressure and temperature of a gas are measured with modest accuracy (about $50\,\mathrm{Pa}$ and $150\,\mathrm{mK}$, respectively, assuming $L_i < 0.5\,\mathrm{m}$), the refractive index will be known well enough that there will be only one value of Δm for which Eq. (2) yields a result consistent with the estimated value. Once Δm is known, Eq. (2) will provide a value for n that is much more accurate than the first estimate.

The length variation factor in Eq. (2) arises primarily from the compressibility of the cavity undergoing a pressure change Δp, and can be related to the bulk modulus K of the cavity material as

$$n \frac{L_i - L_f}{L_i} \approx \frac{\Delta L}{L} = -\frac{\Delta p}{3K}. \tag{3}$$

Note that approximating the left-hand side with $n = 1$ will give errors in refractive index no greater than a few parts in 10^{10}. If desired, this error can be eliminated simply by solving Eq. (2) explicitly for n; the explicit solution for n is not shown here so as to preserve a more heuristic form of the equation, a form that lends itself to the uncertainty analysis soon to follow. Also note that Eq. (2) properly accounts for any length variation of the cavity during the measurement, whether it arises from uniform compressibility as in Eq. (3), from more complex distortions in a cavity made of several different materials, or from some other mechanical instability of the cavity.

We determine the length variation factor using helium, since the refractivity of helium can be calculated from first principles. See [13] for more details on how to correct for errors in a gas refractometer using helium. In practice, we charged the cavities from high vacuum to research purity helium (99.9999%) at a pressure of interest (say 100 kPa), and derived an experimental refractivity using Eq. (2). We compared this experimental refractivity to the theoretical refractivity, and adjusted the value for bulk modulus in Eq. (3) to minimize the difference between the two refractivity values. This process determined K and fixed the length variation factor so that the absolute refractive index of other gases (such as nitrogen and argon) could subsequently be measured by Eq. (2). It is worth noting that a 1% uncertainty in the bulk modulus of the cavity material means an uncertainty of 1×10^{-8} for absolute refractometry. For our cavities we determined $K_{\text{ULE}} = 33.86 \, \text{GPa}$, which differs from the manufacturer's value by slightly less than 1%.

3. Results and Discussion

When considering measurement uncertainties and refractometer performance, it is useful to keep in mind that a change in refractive index of 1×10^{-9} corresponds to a pressure change in atmospheric nitrogen of 0.4 Pa or a temperature change of 1 mK. In terms of frequency measurements, the refractive index change of 1×10^{-9} corresponds to a change in resonant frequency ν_f of 474 kHz. The sensitivity in refractive index to pressure, temperature, and resonant frequency is 8 times smaller for helium. These relationships are expressed as $\frac{d\nu}{\nu} \approx -\frac{dn}{n} - \frac{dL}{L} \approx -\frac{d\rho}{\rho}(n-1)$, where gas density $\rho \propto p/T$ depends upon the pressure p and absolute temperature T of the gas.

A. Measurement Uncertainty

Refractive index measurements are derived from Eq. (2). Ignoring the very small correction factors ε_a and ε_d, the inputs to Eq. (2) are:

- Values such as c and Δm that have no uncertainty.

- The absolute resonant frequencies ν_i and ν_f, which contribute less than 10^{-10} to the uncertainty in refractive index.
- The initial length of the cavity L_i, determined from the measurement of an FSR, $\Delta \nu_{\text{fsr}} = \frac{c}{2L_i}/(1 + \varepsilon_a)$. To prevent uncertainty in L_i from contributing an uncertainty more than $10^{-6} \cdot (n-1)$ to refractive index measurement, it is necessary to measure an FSR to within 1 part in 10^6 and to correct for mirror dispersion within 30% (assuming $L_i > 300 \, \text{mm}$). (We note that L_i could be determined from Eq. (1) with even lower uncertainty; however, our knowledge of $c/(2L_i)$, as determined by an FSR measurement, was only nominally good enough to uniquely identify the mode number m.)
- The correction for length variation, $n(L_i - L_f)/L_i$. The accuracy of refractive index measurement is almost entirely limited by the uncertainty in this term. To first approximation, the value can be estimated using Eq. (3) with the manufacturer's value of bulk modulus; this approximation would result in uncertainty in refractive index of a few parts in 10^8. Much better accuracy—potentially lower than 10^{-9}—can be achieved using helium to correct for vacuum-to-atmosphere compression effects.

Equation (2) is used in two steps to determine the refractive index of a gas. First, it is used to determine the refractive index of helium, and the length variation factor $n(L_i - L_f)/L_i$ is adjusted so as to give the correct (theoretical) value for the refractive index of helium. The standard uncertainties in this process are summarized in the top part of Table 1. Next, this correction for length variation is used in determining the refractive index of an unknown gas sample, the standard uncertainties of which are shown in the bottom part of the table. Uncertainties in the length variation factor, determined via measuring the refractive index of helium, are shown as components 1–8 in the table and are described below.

1. Extrapolation to $t = 0$ h: We cannot perform reliable measurements for several hours after filling the cavities because of temperature transients. After this passage of time, helium will likely have been absorbed into the cavity, changing its length. To correct for this effect, we extrapolate reliable measurements back to $t = 0$ h. This procedure would also correct for any outgassing/permeation that contaminates the helium. More discussion on helium extrapolation follows in the next subsection.

2. Pressure measurement: The value given for pressure measurement uncertainty reflects the combined effects of component uncertainties associated with calibration (0.5 Pa); hysteresis and short-term repeatability (1.5 Pa); temporal drift between the time of calibration and time of use (0.3 Pa); temperature sensitivity of the instrument, which is calibrated at a different ambient temperature than when it is in use (0.2 Pa); and uncertainty in the

gas head correction (0.04 Pa for helium). These have been added in quadrature to give the result shown in Table 1. The uncertainty values quoted are only valid when the barometer is used within a few weeks of the time when it was calibrated and is used to measure pressures that are sufficiently close to calibration points that nonlinearities are not a significant concern.

3. Helium purity: The uncertainty is based on the manufacturers' specifications for purity, recognizing that contaminants will have much higher molar refractivity than does helium. After filling the cavity, contamination might increase over time due to outgassing/permeation, but this is taken into account by extrapolation along with the effect of helium absorption, as mentioned in component 1.

4. Temperature measurement: Similar to pressure measurement, several components have been added in quadrature to give the temperature uncertainty: calibration uncertainty of the reference thermistor (1 mK), drift in calibration (0.5 mK), and possible offset emfs in the thermocouple system as discussed previously (0.5 mK). There is also an uncertainty due to possible unmeasured temperature gradients within the cavities (0.2 mK).

5. Theoretical refractive index of helium: The uncertainty is about 1 part in 10^{10} at a precisely known pressure and temperature [13]. The uncertainty in the calculated refractive index of a helium sample also depends on pressure and temperature measurement uncertainties, as given in components 2 and 4 of Table 1.

6. Cavity stability: The quantity $(L_i - L_f)/L_i$ depends almost entirely on bulk modulus and pressure, and should be reproducible day-to-day. However, we observe two sorts of variation in $L_i - L_f$. The first is a linear drift of about 11 pm/d, which we are confident of correcting to 10%. The second variation in length is related to hysteresis in compressibility: the vacuum resonant frequency changes by 40 kHz after being charged to atmospheric pressure and pumped down to vacuum again. The total instability in cavity length between the beginning and end of a gas measurement is the quadrature sum of these effects, as given in Table 1.

7. Frequency measurement: Uncertainty and instability of the iodine-stabilized laser frequency (5 kHz) affect measurement of ν_i and ν_f, but this contributes a very small uncertainty to the refractive index measurement (10^{-11}). Additionally, since suppressing RAM can be cumbersome, we typically perform gas refractivity measurements without suppression; this contributes a 7 kHz uncertainty in locking to a resonant frequency, which is also nearly negligible.

8. Errors in $c/(2L_i)$: The uncertainty shown in Table 1 for determining $c/(2L_i)$ is for the longer of the two cavities, and its contribution to errors in refractive index scales with gas refractivity. Errors in $c/(2L_i)$ consist of two components. The first is the uncertainty in FSR (61 Hz), which is measured with RAM suppressed. There is a second uncertainty component owing to the mirror dispersion correction, and it is larger for the short cavity than for the long. We assume that we know the mirror dispersion $\alpha \approx 10.5/\nu$ at the design frequency within 15%, based on a model in conjunction with information provided by the manufacturer; we consider the correction for α accurate to 110 Hz. (For the short cavity, errors in $c/(2L_i)$ cause a relative error in the refractive index of nitrogen of 0.11×10^{-9}.)

Adding components 1 through 8 in quadrature, the standard uncertainty in correcting for cavity length variation is 1.4×10^{-9}. To this must be added additional uncertainties when the refractive index of some other gas is measured—the second step of the full measurement process. This second step will be subject to some, but not all, of the sources of uncertainty that have already been discussed. The primary intended use of this refractometer is to measure the refractive index of ambient gas without reference to its temperature and pressure. Pressure and temperature measurements come into play only in as much as they affect the physical length of the cavity via thermal expansion and compressibility; the sensitivity of the FP cavity to variations in these quantities (components 2 and 4 of the table) is so small that the corresponding uncertainties are of negligible importance in the second step. For the

Table 1.   Refractometer Uncertainties and Relative Error in Determining Refractive Index *n* Using Eq. (2) with the Long Cavity

	Component	Measurement Uncertainty	Relative Error ($\times 10^{-9}$)
1	extrapolation to $t = 0$ h	0.4 nm	1.27
2	pressure measurement	1.6 Pa	0.52
3	helium purity	0.0001%	0.24
4	temperature measurement	1.3 mK	0.15
5	theoretical helium n	10^{-10}	0.10
6	cavity stability	12 pm	0.09
7	frequency measurement	9 kHz	0.03
8	errors in $c/(2L_i)$	126 Hz	0.01
	Standard Uncertainty ($k = 1$) for $n(L_i - L_f)/L_i$ Correction		1.41
6b	cavity stability	12 pm	0.09
7b	frequency measurement	9 kHz	0.03
8b	errors in $c/(2L_i)$	126 Hz	0.08
	Standard Uncertainty ($k = 1$) for n of a Dry Gas		1.41

second step there is no analog of uncertainty in components 1, 3, and 5 in the table. Remaining sources of uncertainty are cavity stability (component 6b), frequency measurement (component 7b), and errors in $c/(2L_i)$ (component 8b). In the manner that we have used the FP cavity thus far, uncertainty due to cavity stability is the same in both steps and is only of minor importance. Frequency measurement errors in the second step are the same as shown in component 7 of the first step and are thus nearly negligible. Errors in $c/(2L_i)$ are more important in the second step than in the first; these errors scale proportional to the refractivity $n-1$ and, hence, are approximately 8 times larger for nitrogen or similar gases than for helium. (In principle, we should account for the fact that this error in the second step is completely correlated with the error in the first step, but the correlation has no significant impact on the final result.) In summary, these additional uncertainty components associated with the second measurement step add essentially nothing to the overall uncertainty budget for refractive index measurement. The overall standard uncertainty in measuring a dry gas at atmospheric pressure is 1.4×10^{-9} (or an expanded uncertainty of 2.8×10^{-9}).

This uncertainty will be significantly larger for other modes of operation. Ideally, we would like to utilize the FP cavity for long periods of time without a vacuum system, and under these circumstances the cavity stability might be the dominant uncertainty factor. Although we have not yet carefully characterized the long-term stability of the cavity, it appears that the long-term drift in ν_i is probably on the order of 1.2 MHz per month (corresponding to a cavity length shrinking by 0.3 nm per month). This would cause a refractive index error of 3 parts in 10^8 per year, if the cavity were not recalibrated (that is, ν_i remeasured). Origins of drift in ν_i may be aging of the ULE or aging and/or contamination of the mirror coatings (which might change mirror phase shifts and thus change the effective cavity length). The drift in ν_i of our cavity appears between 1.5 and 4 times larger than one ULE cavity previously reported [15], and further study is required before we can comment on the long-term linearity (and, thus, how well drift in ν_i might be corrected for via extrapolation).

In another mode of operation, we have also used the refractometer to measure the molar refractivity of pure gases or, equivalently, the refractive index at specified temperatures and pressures. Temperature and pressure measurements again become important for this measurement: the bottom part of Table 1 must include uncertainty components 2b and 4b, the contribution of which to the relative error in refractive index would be increased by a factor of approximately 8 over components 2 and 4 (the respective components are partially correlated). This gives an expanded uncertainty of $< 9 \times 10^{-9}$ ($k = 2$) in the refractive index reference values for nitrogen and argon at specified temperature and pressure.

B. Refractometer Performance

As already mentioned, one problem with correcting for compression in a ULE cavity is the absorption of helium into the glass. This absorption has the effect of lengthening the cavity, thereby introducing uncertainty into the determination of the length variation factor of Eq. (3). Figure 2 shows the temperature, pressure, and frequency dynamics for a helium correction, where the resonant frequency of the cavity ν_{meas} has been corrected for changes in helium density ρ, that is $\frac{d\nu}{\nu} \approx -\frac{d\rho}{\rho}(n-1)$, and

$$\nu_{\mathrm{corr}} = \nu_{\mathrm{meas}} + \nu_{\mathrm{nom}}\left[\frac{p}{p_{\mathrm{nom}}} \cdot \frac{T_{\mathrm{nom}}}{T} - 1\right](n_{\mathrm{nom}} - 1), \quad (4)$$

where p is pressure, T is absolute temperature, and nominal values were used for laser frequency ν_{nom}
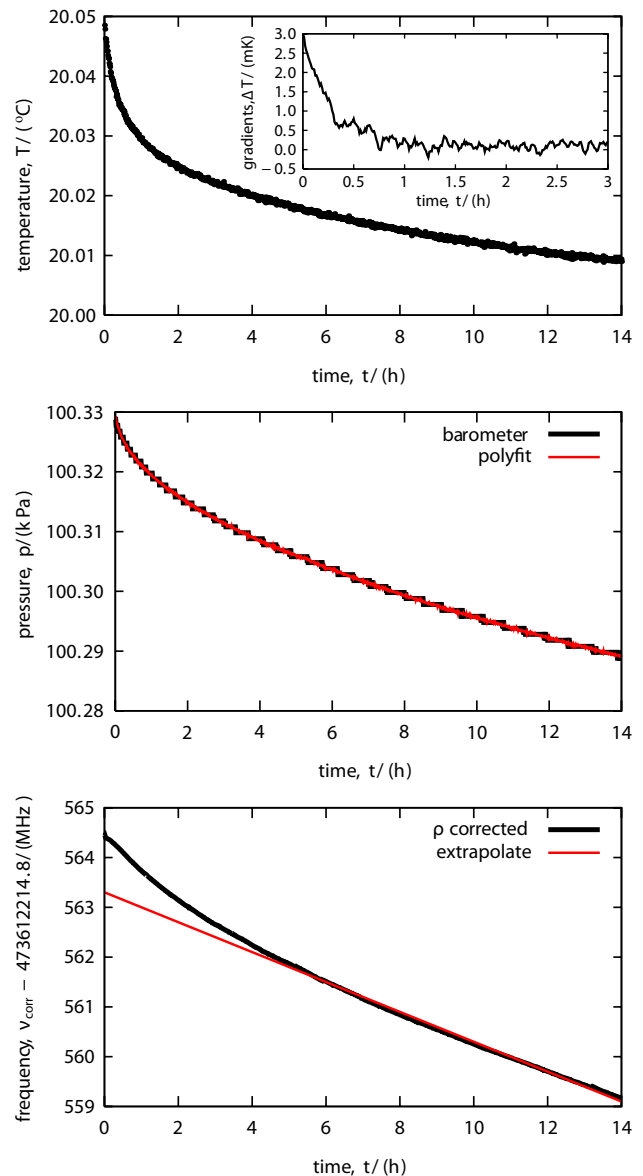

Fig. 2. (Color online) Temperature, pressure, and (density corrected) frequency dynamics for a helium correction of the long ULE cavity.

and refractivity $n_{nom} - 1$. As can be seen in Fig. 2, the gas was cooling toward the normal operating temperature, following the temperature jump associated with adding gas to the chamber. This cooling (approximately 40 mK decrease in temperature) caused a decrease in pressure, but after taking this into account, helium absorption into the ULE during 14 h of exposure caused a drop in pressure of almost 30 Pa. This absorption of helium caused a lengthening of the cavity, as reflected in the decreasing absolute resonant frequency ν_{corr} of the long cavity at a rate of 300 kHz/h (that is, a length increase of 0.2 nm/h). If outgassing were a problem, it would also cause the corrected frequency to decrease, but the effect seen in Fig. 2 can be attributed entirely to helium absorption and lengthening because the rate of frequency decrease was consistent with the 4.7 MHz decrease observed in the initial vacuum frequency ν_i before and after 14 h of exposure to 100 kPa helium. The time constant for helium release from the cavities was 155 h, and this estimate was based on the apparent increase in the outgassing/permeation rate of the evacuated chamber after the cavities had been exposed to helium. It is worth restating what is happening during a helium correction: (a) the pressure-induced length distortion we are trying to correct for occurs within an hour or so of going from vacuum to atmospheric pressure and contrariwise, but (b) when exposed to atmospheric helium, the physical length of the cavity begins increasing as a result of helium absorption into the ULE, and (c) this length increase due to helium absorption is obvious because after exposure to atmospheric helium and when pumped down to vacuum, it takes several days for the cavity to return to its original length.

In order to determine experimental helium refractivity accurately with Eq. (2) and, hence, correct for pressure distortion (length variation), the value of ν_{corr} must be known at time $t = 0$ h, the time immediately after charging to 100 kPa helium (before helium absorption and cavity lengthening). The value of ν_{corr} shown in Fig. 2 at $t = 0$ h is not necessarily reliable, however, because of poorly understood transient phenomena that occur when the cavities are filled. (Transient phenomena are also evident in nitrogen and argon data, where they are not entangled with the effects associated with gas infusion that occur for the helium data.) Some of the nonlinear temporal variations for $t < 4$ h might be attributed to transient temperature gradients between the ends of a cavity, as shown in the inset at the top of Fig. 2 (the difference between the readings of two thermocouples), but it is difficult to quantitatively explain all of the nonlinearity in this manner. Consequently, it is not clear if it is better to use the observed value for ν_{corr} at $t = 0$ h or to extrapolate linearly to $t = 0$ h based on the reliable data beyond 4 h. Because of this ambiguity, we assign a standard uncertainty of 600 kHz (0.4 nm) to this $t = 0$ h extrapolation and helium correction step. We also note that this length variation correction has been performed with

research purity helium from two different manufacturers, and the agreement in the estimated bulk moduli for ULE was within 0.08%.

In contrast to helium, the absolute resonant frequency for atmospheric nitrogen corrected to fixed pressure and temperature was stable and fluctuated around its mean with a standard deviation $\sigma = 57$ kHz, as shown in Fig. 3. As suggested by the $\pm 2\sigma$ limits on the plot, the refractometer had a resolution within 1 part in 10^9 (for $t > 10$ h). A good part of the fluctuations evident in ν_{corr} is related to corrections for nitrogen density from Eq. (4): the barometer and thermometer had resolutions of 0.1 Pa and 0.4 mK, respectively; fluctuations of these orders in pressure and temperature data introduced fluctuations to density corrected frequency at the hundred kilohertz level. There was no evidence that nitrogen or argon interacted with the cavity mirrors or spacer length at more than the 2×10^{-10} level: the absolute resonant frequencies of both cavities (for $t > 10$ h) were very stable with gas pressure of 100 kPa (as can be deduced from Fig. 3), and the vacuum resonant frequencies before and after 40 h of exposure to these gases did not change by more than 100 kHz. The intercavity beat frequency after charging to nitrogen at
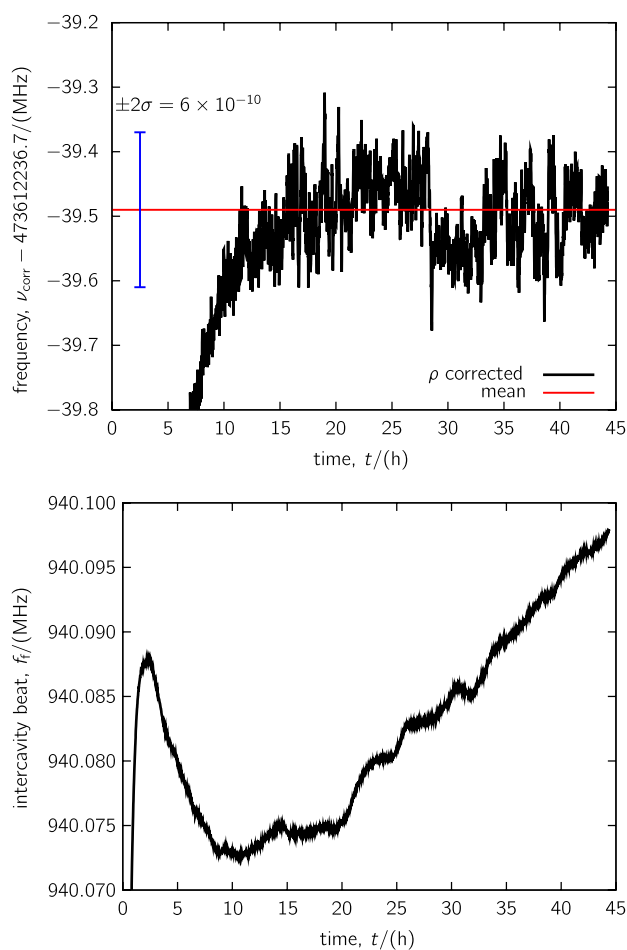

Fig. 3. (Color online) Absolute resonant frequency (density corrected) of the short cavity, and beat frequency between two cavities, after charging to 100 kPa nitrogen.

100 kPa is also shown in Fig. 3, and it fluctuated by roughly 30 kHz over 40 h. Since at fixed pressure $\frac{d\nu}{\nu} \approx \frac{dT}{T}(n-1)$, the 30 kHz fluctuations indicate that temperature fluctuations between the two cavities were less than 70 μK. It is also worth noting that the Allan deviation of the intercavity beat was less than 40 Hz with an averaging time of 100 s, which is only 4 times less stable than the beat between two lasers locked to adjacent modes of the same cavity; the Allan deviation of the intercavity beat with 1 h averaging was 1 kHz.

A pertinent experimental diagnostic is how well the cavities "track" each other going from vacuum to atmospheric pressure. If both cavities have the same bulk modulus, the rf intercavity beat f_f between the two cavities at a final pressure can be related to the intercavity beat f_i at an initial pressure by

$$f_f = \frac{f_i + \left(\Delta m^{\text{long}} \frac{c}{2L_i^{\text{long}}} - \Delta m^{\text{short}} \frac{c}{2L_i^{\text{short}}} \right)}{1 + \frac{\Delta n}{n_i}}, \quad (5)$$

where Δn and Δm are the changes in refractive index and cavity mode number, respectively, going from an initial pressure to a final pressure, n_i is the refractive index at an initial pressure, and, in this case, f_f and f_i refer to the intercavity beats of the long cavity minus the short cavity resonant frequencies at final and initial pressures, respectively. Small corrections (<10 kHz) due to mirror dispersion and diffraction have been ignored in Eq. (5), but mirror dispersion was taken into account when determining $c/(2L_i)$ from the FSR. In this way, measured intercavity beats can be compared to calculations (expected values) from Eq. (5), and the failure of the cavities to track one another going from vacuum to atmospheric pressure can be assessed. In many tests at different pressures of nitrogen and argon, we did not observe failures in tracking greater than 200 kHz, which corresponds to a disagreement in refractive index of only 5×10^{-10} between the two cavities. The fact that the cavities track each other to this level isolates uncertainty arising from errors in measuring cavity vacuum lengths and temperature gradients, because: (a) with $\Delta m^{\text{long}} \approx 300$ going from vacuum to 100 kPa nitrogen, an error in $c/(2L_i^{\text{long}})$ of 1 kHz would give a tracking error of 300 kHz, and (b) a steady-state gradient of 1 mK between the cavities would give a tracking error of 500 kHz. This tracking test also verifies that there are no anomalous distortions greater than 5 parts in 10^{10} in either cavity as a function of pressure.

C. Refractivity of Nitrogen and Argon

We measured the refractivities of nitrogen and argon gases with $p = (100 \pm 0.5)$ kPa and $T = (20 \pm 0.005)$ °C. These values were scaled to 100 kPa and 20 °C and averaged to give the results shown in the first row of Table 2. From these refrac-

tivity values we can compute molar refractivities using the method of [13]. The calculations rely on density virial coefficients from Dymond *et al.* [21] and refractivity virial coefficients from Achtermann *et al.* [22]. This procedure gave a molar refractivity of 4.44585 cm³/mol for nitrogen and 4.19545 cm³/mol for argon. These molar refractivity values have an expanded uncertainty of 1.2×10^{-4} cm³/mol, primarily arising from uncertainty in the refractive index measurements, but also including a nonnegligible contribution from uncertainty in the virial coefficients. Also shown in Table 2 are corresponding results obtained using the molar refractivity values given by Birch [23], Hou and Thalmann [24], and Achtermann *et al.* [22]. Except for the argon measurements of Achtermann *et al.* (which claim a much lower uncertainty than is assigned to the corresponding nitrogen results), the results in the table are at least nominally consistent within the stated uncertainties. Our results for nitrogen are also consistent with higher uncertainty measurements that were previously carried in our laboratory [13].

As mentioned above, the expanded uncertainty of our reference values is $<9 \times 10^{-9}$ ($k = 2$), which is nearly 5 times more accurate than Birch. These reference value measurements have been repeated on different gas cylinders from different manufacturers, where the gas grades were ultrahigh purity (99.9995%) at minimum, and we have not observed a disagreement between refractive index calculations of more than 2×10^{-9}, which is within $\sigma/2$ of our stated uncertainty budget. As discussed in the previous subsection, the agreement in refractive index between our long and short cavities (cavity tracking) in a single run was better than 5 parts in 10^{10}.

D. Effect of Humidity

The refractometer performance degrades when attempting to measure the refractive index of moist air. For the tracking test described in Eq. (5), the cavities failed to track each other by about 10 MHz when exposed to air of humidity 40% relative humidity (RH). This effectively means that if used in a typical lab environment, the cavities would give answers for refractive index that differ by 2.1×10^{-8}. The most likely interpretation of this result is that humidity causes a 7 nm shift in the apparent position of the surfaces of the mirrors. This shift of position is relatively more important for a short cavity than for a long one; we expect the error to be inversely proportional to cavity length. The 10 MHz failure to track

Table 2. Derived Reference Values for the Refractivities of Nitrogen and Argon for $p = 100$ kPa, $T = 20$ °C, and $\lambda = 633$ nm

	$(n-1) \times 10^8$	
	Nitrogen	Argon
This work	27368.2 ± 0.9	25838.9 ± 0.9
Birch	27368 ± 4	25838 ± 4
Hou and Thalmann	27367 ± 4	25839 ± 4
Achtermann *et al.*	27372 ± 3	25842 ± 1

would then be interpreted as a 7.7 MHz error in the long cavity and a 17.7 MHz error in the short cavity, corresponding to errors in refractive index of 1.6×10^{-8} and 3.7×10^{-8}, respectively. The 10 MHz tracking failure going from vacuum to 40% RH atmospheric air manifested itself within 2 h of exposure, and did not fluctuate by more than 100 kHz over 125 h in air; that is, the response of the cavities to moisture appeared rapid and without long-term drift.

The effect of increasing and decreasing humidity on cavity tracking is shown in Fig. 4. Silica gel desiccant and saline solution were used to control the humidity of the air in the chamber from 10% RH to 70% RH. A dew point hygrometer was used to occasionally measure humidity at the cavities; the hygrometer could not be turned on continuously because it generated large temperature gradients. As evident in Fig. 4, the disagreement in the refractive index of air between the cavities is clearly humidity dependent. Disagreement between the cavities increases fairly linearly with increasing humidities less than 35% RH; from 35% RH to 70% RH, the fluctuation in refractive index disagreement is about 1×10^{-9}. The trend is repeatable whether increasing or decreasing humidity, and, again, the response of the cavities to changing humidity was rapid.

There are at least three possible humidity-related mechanisms that might cause disagreement between the cavity refractometers: (a) adsorbed water monolayers on the mirror surface, (b) meniscus forces distorting the mirror surface and/or cavity length, and (c) water penetration into the mirror quarterwave stack. When we model our mirrors with a 10 nm layer (30 monolayers) of $n = 1.33$ adsorbed onto the front surface of the mirror, we calculate only a 25 pm apparent shift in the front surface of the mirror at the design wavelength. (The surprisingly small shift caused by a thin contaminate layer at the design wavelength is discussed, for example, in [25].) Taking into account that we operate 11 nm away from the mirror design wavelength, this apparent shift is still
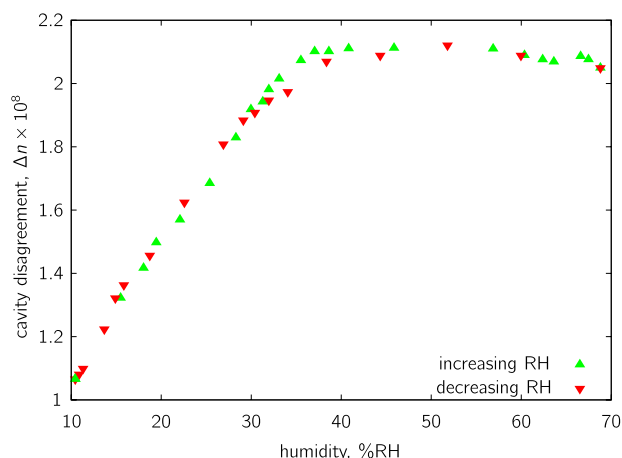

Fig. 4. (Color online) Disagreement in the refractive index of air between the cavities as a function of relative humidity.

less than 70 pm. And so, with two mirrors forming a cavity, it seems unreasonable to attribute the inability of the cavities to track one another within 7 nm to adsorbed water monolayers. Meniscus force might matter if there were a spacing of a few nanometers circumferential to the optical contact between the mirrors and spacer. Finite element modeling we have done suggests that 5 N of meniscus force around the region of optical contact would cause bending of the mirror surface as large as 3 nm. However, the manufacturer of our cavities assures us that, apart from a 0.5 mm spacing around the mirror, the mirror substrate and spacer are completely and monolithically bonded; meniscus force would be negligible in a spacing 0.5 mm wide. As for the mirror quarterwave stack, the cavity manufacturer also assures us that the mirrors are ion-beam sputtered, and ion-beam sputtered coatings are reputed to have minimal sensitivity to water penetration and humidity. Given that each of the three possible explanations outlined above appear unlikely, at the present time we do not understand why our cavities are sensitive to humidity at the 10^{-8} level, and we intend to investigate humidity effects further in future work.

E. Comparison with Old Cavities

We had the capability of comparing these "new" cavities to "old" cavities used in a previous study [13]. The point of interest in this comparison is that the new and old cavities have significant differences in manufacture. Note that apart from this final subsection, the rest of this paper has exclusively dealt with the new cavities.

The old cavity (manufactured in 1998) had several undesirable characteristics, including: a Zerodur [14] spacer with fused silica mirror substrates, and the mirrors were rf magnetron sputtered to low finesse (140) and had higher uncertainty in dispersion. The old cavity had a thermal expansion coefficient of 5×10^{-8} K^{-1} at 20 °C, which is about 16 times larger than the coefficient of the new cavity, but this did not contribute significant uncertainty to gas refractivity measurement. The old cavity ($L = 453$ mm) exhibited a dimensional stability of 0.7 nm/d and hysteresis in compressibility contributed a 0.5 nm uncertainty in cavity length; both these effects mean the old cavity is about 14 times less stable than the new cavity. The best that could be done in deriving L_i with an FSR measurement plus dispersion correction contributed an uncertainty of $2.3 \times 10^{-6} \cdot (n-1)$ toward gas refractive index, which is about 8 times worse than the new cavity. However, since only the mirrors (fused silica) were susceptible to helium absorption, the length of the old cavity appeared uninfluenced by helium exposure at the 0.1 nm level (and the sensitivity of cavity length to helium absorption may have been less, but we could not assess it any better owing to the poor dimensional stability of the old cavity). Given the poor dimensional stability of the old cavity, this reduced sensitivity to helium absorption is of little benefit, and the

standard uncertainty of the old cavity is 1.9×10^{-9} (confer with Table 1) when measuring the refractive index of a dry gas on a tens-of-hours time scale.

After correcting for the length variation factor with helium, the old cavity agrees with the new cavity to within 1.5×10^{-9} when measuring the refractive index of nitrogen or argon at atmospheric pressure. The tracking test of Eq. (5) gives an offset of 185.7 MHz between the cavities at atmospheric pressure, but the value of this offset is repeatable within 500 kHz. This offset in tracking is expected since the old and new cavities are made from different materials (different bulk moduli) and their respective length variation factors differ by 3.9×10^{-7}. The repeatability in the tracking offset and the agreement in refractive index between the old and new cavities gives us good confidence that helium gas can be used to correct for compressibility distortions in a refractometer to the 10^{-9} level, independent of the refractometer manufacture.

4. Conclusion

We have reported an FP cavity based refractometry system capable of measuring the absolute refractive index of dry gas with an expanded uncertainty $<3 \times 10^{-9}$ ($k = 2$). The chief contribution to this uncertainty is the compressibility correction with helium: our ULE cavities absorb helium and we have nonlinear lengthening behavior immediately after helium exposure, which limits how confidently we can determine the length variation factor. Nevertheless, we can be reasonably confident of results at the claimed uncertainty level, because we have achieved agreement at the 1.5×10^{-9} level between three different cavities—one of which had significantly different length, and one of which was built of different materials. We have improved upon and reported reference values for the refractive index of nitrogen and argon ($p = 100 \, \text{kPa}$, $T = 20 \, °\text{C}$, and $\lambda = 632.8 \, \text{nm}$), which will be useful in calibrating less accurate refractometers. We have also supplied values for the molar refractivity of these gases, from which anyone with a comparable pressure measurement capability (and moderately good temperature measurement) can achieve better than 1 part in 10^8 uncertainty in the refractive index of an atmospheric nitrogen or argon environment. The cavities have a sensitivity to moisture at the 2×10^{-8} level, which we can not fully explain. Future work will determine how well these moisture-related errors can be corrected.

References and Notes

1. B. Edlén, "The refractive index of air," Metrologia **2**, 71–80 (1966).
2. K. P. Birch and M. J. Downs, "An updated Edlén equation for the refractive index of air," Metrologia **30**, 155–162 (1993).
3. P. E. Ciddor, "Refractive index of air: new equations for the visible and near infrared," Appl. Opt. **35**, 1566–1573 (1996).
4. G. Bönsch and E. Potulski, "Measurement of the refractive index of air and comparison with modified Edlén's formulae," Metrologia **35**, 133 (1998).
5. J. A. Stone and J. H. Zimmerman, "Refractive index of air calculator," http://emtoolbox.nist.gov/Wavelength/Abstract.asp.
6. W. T. Estler, "High-accuracy displacement interferometry in air," Appl. Opt. **24**, 808–815 (1985).
7. T. Doiron and J. Stoup, "Uncertainty and dimensional calibrations," J. Res. Natl. Inst. Stand. Technol. **102**, 647–676 (1997).
8. J. S. Beers and W. B. Penzes, "The NIST length scale interferometer," J. Res. Natl. Inst. Stand. Technol. **104**, 225–252 (1999).
9. M. Andersson, L. Eliasson, and L. R. Pendrill, "Compressible Fabry–Perot refractometer," Appl. Opt. **26**, 4835–4840 (1987).
10. M. L. Eickhoff and J. L. Hall, "Real-time precision refractometry: new approaches," Appl. Opt. **36**, 1223–1234 (1997).
11. N. Khélifa, H. Fang, J. Xu, P. Juncar, and M. Himbert, "Refractometer for tracking changes in the refractive index of air near 780 nm," Appl. Opt. **37**, 156–161 (1998).
12. R. W. Fox, B. R. Washburn, N. R. Newbury, and L. Hollberg, "Wavelength references for interferometry in air," Appl. Opt. **44**, 7793–7801 (2005).
13. J. A. Stone and A. Stejskal, "Using helium as a standard of refractive index: correcting errors in a gas refractometer," Metrologia **41**, 189–197 (2004).
14. Any mention of commercial products is for information only; it does not imply recommendation or endorsement by NIST nor does it imply that the products mentioned are necessarily the best available for the purpose.
15. L. Marmet, A. A. Madej, K. J. Siemsen, J. E. Bernard, and B. G. Whitford, "Precision frequency measurement of the $^2S_{1/2} - {}^2D_{5/2}$ transition of Sr^+ with a 674 nm diode laser locked to an ultrastable cavity," IEEE Trans. Instrum. Meas. **46**, 169–173 (1997).
16. A. Takahashi, "Long-term dimensional stability and longitudinal uniformity of line scales made of glass ceramics," Meas. Sci. Technol. **21**, 105301 (2010).
17. R. W. Fox, "Temperature analysis of low-expansion Fabry–Perot cavities," Opt. Express **17**, 15023–15031 (2009).
18. M. S. Taubman and J. L. Hall, "Cancellation of laser dither modulation from optical frequency standards," Opt. Lett. **25**, 311–313 (2000).
19. P. Egan and J. A. Stone, "Temperature stabilization system with millikelvin gradients for air refractometry measurements below the 10^{-8} level," NCSLI Measure: J. Measure Sci. **6**, 40–46 (2011).
20. J. R. Lawall, "Fabry–Perot metrology for displacements up to 50 mm," J. Opt. Soc. Am. A **22**, 2786–2798 (2005).
21. J. D. Dymond, K. N. Marsh, R. C. Wilhoit, and K. C. Wong, "Virial coefficients of pure gases and mixtures," in *Landolt–Börnstein: Group IV Physical Chemistry* (Springer–Verlag, 2002), Vol. 21A.
22. H. J. Achtermann, G. Magnus, and T. K. Bose, "Refractivity virial coefficients of gaseous CH_4, C_2H_4, C_2H_6, CO_2, SF_6, H_2, N_2, He, and Ar," J. Chem. Phys. **94**, 5669–5684 (1991).
23. K. P. Birch, "Precise determination of refractometric parameters for atmospheric gases," J. Opt. Soc. Am. A **8**, 647–651 (1991).
24. W. Hou and R. Thalmann, "Accurate measurement of the refractive index of air," Measurement **13**, 307–314 (1994).
25. W. Lichten, "Precise wavelength measurements and optical phase shifts. I. General theory," J. Opt. Soc. Am. A **2**, 1869–1876 (1985).